CITIUS:
an IR-XUV light source for fundamental and applied ultrafast science

C. Grazioli[1,2], C. Callegari[2], A. Ciavardini[3], M. Coreno[4,2], F. Frassetto[5], D. Gauthier[1,2], D. Golob[6], R. Ivanov[1,2], A. Kivimäki[7], B. Mahieu[2,8], Bojan Bučar[9], M. Merhar[9], P. Miotti[5], L. Poletto[5], E. Polo[10], B. Ressel[1], C. Spezzani[2], and G. De Ninno[1,2]

1. Laboratory of Quantum Optics, University of Nova Gorica, Nova Gorica, Slovenia
2. Elettra Sincrotrone Trieste, Trieste, Italy
3. Sapienza University, Rome, Italy
4. Institute of Inorganic Methodologies and Plasmas (CNR-IMIP), Montelibretti, Roma, Italy
5. Institute of Photonics and Nanotechnologies (CNR-IFN), Padova, Italy
6. Kontrolni Sistemi d.o.o., Sežana, Slovenia
7. Institute of Materials Manufacturing (CNR-IOM), TASC Laboratory, Trieste, Italy
8. Service des Photons Atomes et Molécules, Commissariat à l'Energie Atomique, Centre d'Etudes de Saclay, Bâtiment 522, 91191 Gif-sur-Yvette, France
9. Laboratory of Mechanical Processing Technologies, University of Ljubljana, Slovenia
10. Institute of Organic Synthesis and Photoreactivity (CNR-ISOF), Ferrara, Italy

(Dated: December 29, 2013)

We present the main features of CITIUS, a new light source for ultrafast science, generating tunable, intense, femtosecond pulses in the spectral range from IR to XUV. The XUV pulses (about 10^5-10^8 photons/pulse in the range 14-80 eV) are produced by laser-induced high-order harmonic generation in gas. This radiation is monochromatized by a time-preserving monochromator, allowing one also to work with high-resolution bandwidth selection. The tunable IR-UV pulses (10^{12}-10^{15} photons/pulse in the range 0.4-5.6 eV) are generated by an optical parametric amplifier, which is driven by a fraction of the same laser pulse that generates high order harmonics. The IR-UV and XUV pulses follow different optical paths and are eventually recombined on the sample for pump-probe experiments. We also present the results of two pump-probe experiments: with the first one, we fully characterized the temporal duration of harmonic pulses in the time-preserving configuration; with the second one, we demonstrated the possibility of using CITIUS for selective investigation of the ultra-fast dynamics of different elements in a magnetic compound.

PACS numbers:

I. INTRODUCTION

Thanks to advances in laser science occurred over the last two decades, it is now possible to produce VUV and soft X-ray pulses in the femtosecond range, using different approaches: laser-induced high-order harmonic generation in gas (HHG), free-electron lasers, and laser slicing at synchrotron beamlines [1]. The femtosecond revolution triggered by HHG sources opened up the field of femtochemistry [2], making intramolecular motion of atoms accessible to experimentalists. In fact, HHG sources are very powerful tools, which may be used to capture the fastest electron dynamics in atoms, molecules, and materials and to investigate nanostructures relevant to magnetic storage, nanoscience and nanotechnology, energy transport and harvesting, thermal management, nanoscale imaging, and more [3, 4]. In HHG, noble-gas atoms interact with an intense laser field and emit light at the harmonics of the latter. The process can be described by means of a semi-classical "three step model" [5]. In the first step, a bound electron is extracted from a gas atom under the action of the laser field; in the second step, the electron undergoes an oscillating motion imposed by the laser field; in the third step, the electron collides back with the parent ion. As a result, laser harmonics are emitted up to wavelengths extending into the soft X-ray regime, and dropping quickly at some cutoff energy [6–8].

Since the electron dynamics in atomic, molecular or more complex systems occurs at timescales ranging from hundreds of femtoseconds down to tens of attoseconds, HHG sources provide an ideal tool to study, and possibly control, the interactions between charge, lattice, orbital, and spin dynamics in a chemical reaction.

In 2008, a new project has been funded in the framework of the Cross-border cooperation program between Italy and Slovenia 2007-2013 [9]. Project's main objective is to set up a state-of-the-art HHG light source, named CITIUS, at the University of Nova Gorica (Slovenia). As

detailed in the following, the originality of our source with respect to other HHG facilities [10–13] relies on the implementation of an innovative monochromator, allowing one to work in time-preserving or high-resolution regimes, as well as on the use of an optical parametric amplifier, allowing one to generate fully tunable radiation in the IR-UV spectral range. The combination of these tools provides users with the possibility to carry out two-color experiments in which both the pump and the probe can be tuned at the desired wavelength, while maintaining a high temporal resolution. Part of the envisaged scientific program will be connected to that developed at the Low-Density Matter beamline at the FERMI@Elettra free-electron laser [14].

In this paper, we first provide a technical description of the source CITIUS, and then report the results of two proof-of-principle pump-probe experiments, namely the characterization of the temporal structure of HHG pulses, and the selective investigation of the ultra-fast dynamics of different elements in a magnetic compound.

II. THE LASER SYSTEM AND THE BEAMLINE

The CITIUS laser system and the beamline are schematically shown in Fig.1.

The laser system comprises a commercial amplifier Legend Elite Duo and an optical parametric amplifier OPerA (OPA), both produced by Coherent Inc. The amplifier is seeded by a Micra oscillator (wavelength: 800 nm, spectral bandwidth about 100 nm, power about 380 mW) and includes two amplification stages: a regenerative amplifier (EVO 30), pumped by an Evolution 30 laser (frequency-doubled Q-Switched Nd:YLF laser), and a single-pass amplifier (EVO HE), pumped by an Evolution HE laser (frequency-doubled Q-Switched Nd:YLF laser). The system can be operated at four different repetition rates: 100 Hz, 1 kHz, 5 kHz and 10 kHz. At 5 kHz, which is the currently adopted repetition rate, it generates pulses carrying about 3.1 mJ, with a duration of about 35 fs, centered at 805 nm. Two thirds of the energy is used for generating XUV pulses through HHG, one third as a pump for the OPA, or directly in combination with the HHG beam for pump-probe experiments. The OPA produces tunable radiation in the range between 0.4 eV and 5.6 eV, with variable energy per pulse (from few to hundreds of microjoules). The optical elements transporting the fundamental have a roughness equal to $\lambda/6$.

The beamline includes a high-vacuum section, through which the XUV beam propagates, and a section in air, used to transport the IR-UV light generated by the OPA. The XUV part comprises a HHG generation chamber and a monochromator. The laser is focused in the generation chamber (using the lens L1, see Fig.1), where it interacts with a noble gas of choice (Ar or Ne, for the reported experiments) contained in a cell, generating the high-order harmonics. The harmonic generation efficiency can be

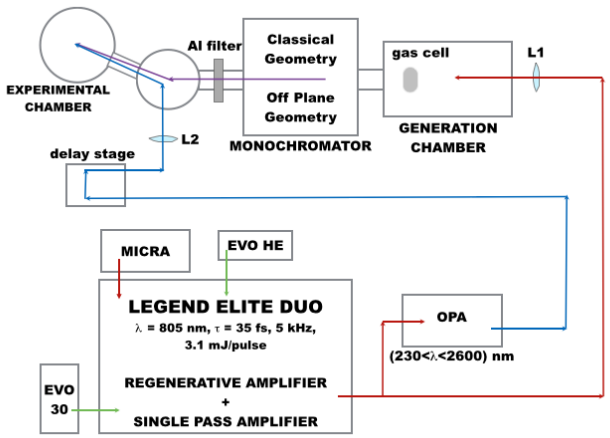

FIG. 1: Layout of the CITIUS source including the laser system, the harmonic generation chamber, the monochromator, the recombination chamber, the delay line and the experimental chamber. The light generated by the Legend amplifier is separated in two parts by the beam splitter BS. The reflected part (about two thirds of the incoming beam) is focused (with the lens L1) into the generation chamber, where it is used for HHG. The HHG beam is monochromatized, filtered (in order to eliminate the residual IR beam) and sent into the refocusing chamber. From there, it is finally focused into the experimental chamber, using a toroidal mirror. The part of laser beam transmitted by BS is either sent to the OPA, or transmitted directly. The OPA/direct beam is then sent through a delay line, focused (with the lens L2) and reflected (by a planar mirror located in the refocusing chamber) into the experimental chamber. In the monochromator, CG stands for "classical geometry" configuration, used for high-energy resolution measurements, while OPG represents the "off-plane geometry" configuration, used for high-temporal resolution measurements (see Fig.2 for details about the two configurations).

optimized by varying the laser intensity, the gas pressure (typically, of the order of 10^{-3} mbar) and the relative position of the laser focus within the cell.

The grating monochromator, whose scheme is shown in Fig.2, was developed by CNR-IFN Padova (Italy). It has been designed to select one single harmonic, or a sub-band of it, in the spectral range between 250 and 12 nm (5-100 eV). A principal aim of the design of any grating monochromator for ultrafast pulses is to minimize the stretch of the pulse duration at the ouput that is due to the pulse front-tilt introduced by the grating. The CITIUS monochromator differs from other systems for the spectral selection of high-order harmonics [15–17], in that it adopts a single-grating design with a double-stage configuration [18, 19]. Based on the experimental requirements, the user can use either a grating stage in the off-plane geometry (OPG) with minimum pulse-front tilt for ultrafast response (i.e., few tens of femtoseconds) at the expense of energy resolution, or a grating stage in

the classical geometry (CG) for high-energy resolution, albeit with long temporal response (i.e., several hundreds of femtoseconds). As shown in Fig.2, a first toroidal mirror collimates the light coming from the generation chamber and deflects it to the grating stages, OPG or CG. The diffracted light is then refocused by a second toroidal mirror onto the exit slit. The characteristics of the OPG and CG gratings are reported in Table I..

TABLE I: Characteristics of the monochromator gratings. The energy resolution has been calculated on a 100-μm-wide exit slit.

Off-plane geometry (OPG)	
G200 (groove density: 200gr/mm)	
Spectral region	100-250 nm (12-5 eV)
Energy resolution	0.1 eV @ 10 eV
G400 (groove density: 400gr/mm)	
Spectral region	27-100 nm (45-12 eV)
Energy resolution	0.2 eV @ 20 eV
G600 (groove density: 600gr/mm)	
Spectral region	12-40 nm (100-30 eV)
Energy resolution	0.5 eV @ 40 eV
Classical geometry (CG)	
G300 (groove density: 300gr/mm)	
Spectral region	80-250 nm (12-5 eV)
Energy resolution	10 meV @ 10 eV
G600 (groove density: 600gr/mm)	
Spectral region	50-100 nm (25-12 eV)
Energy resolution	20 meV @ 20 eV
G1200 (groove density: 1200gr/mm)	
Spectral region	30-60 nm (41-21 eV)
Energy resolution	40 meV @ 40 eV

The branch transporting the OPA/IR beam includes a delay line, allowing one to control the optical path difference between the pump and probe beams with submicron precision. The OPA/IR beam is refocused by a lens (L2 in Fig.1) and intercepted by a flat mirror (BK7, high-reflectivity, replaceable according to the specific wavelength in use) hosted in the recombination chamber. At the exit of the monochromator, the XUV beam passes through a 200 nm thick Al filter (to stop the residual IR seed laser) and enters the recombination chamber. The chamber hosts a toroidal mirror (Si:Au coated, with 1200 mm focal length) to refocus the monochromatized XUV light at the sample position. The mirror sits in a two-axes motorized mount, to guarantee (with micrometric precision) a perfect spatial overlap between the pump and probe beams onto the sample. The pump and probe beams impinge onto the sample in an almost collinear geometry in order to minimize the temporal resolution spread due to the lateral spots dimensions.
Each chamber of the beamline is pumped by a turbo pump and a connected fore-vacuum scroll pump and can be isolated in sections by means of manual valves. The

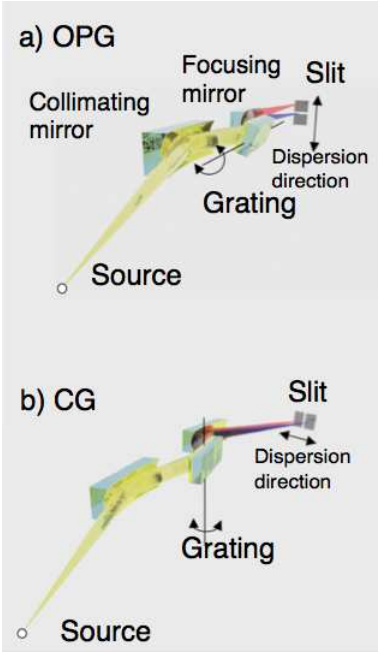

FIG. 2: Light paths inside the monochromator: a) off plane geometry (OPG); b) classical geometry (CG).

pressure in the HHG chamber during generation is typically in the range of 10^{-3}mbar; however a suitable set of pinholes allows to preserve the vacuum in the beamline. Typical pressures in the monochromator and in the refocussing chambers are, respectively, in the range of 10^{-7}mbar and 10^{-9}mbar. A further set of pinholes, placed after the refocussing section, preserves UHV vacuum in the experimental chambers, when needed. In order to achieve a beam stability of the order of few tens of micrometers and temporal resolution of the order of few tens of picoseconds, the laboratory floor has been isolated so to dump environmental vibrations.

III. HHG PERFORMANCE

We measured the quality and sizes of the XUV spots after the refocalization chamber at 1200 mm from the center of the refocalizing mirror, where the XUV spot is focused. In Fig.3 left, we present the XUV spot of the 23$^{\text{rd}}$ harmonic generated in Ar. The OPG G400 grating was used, with a slit aperture of 200 μm. The measured spot size is 140 μm x 220 μm (FWHM). In Fig.3 right, we present the XUV spot of the 25$^{\text{th}}$ harmonic generated in Ar. In this case, the CG G1200 grating was used, with a slit aperture of 200 μm. The obtained spot size is 220 μm x 120 μm (FWHM). The OPA beam focusing can be adjusted in order to obtain a spot approximately twice as big. This ensures a homogeneous excitation of the probed area. The energy density of the IR-UV at the interaction point has been estimated to be of the order of 10 mJ/cm^2.

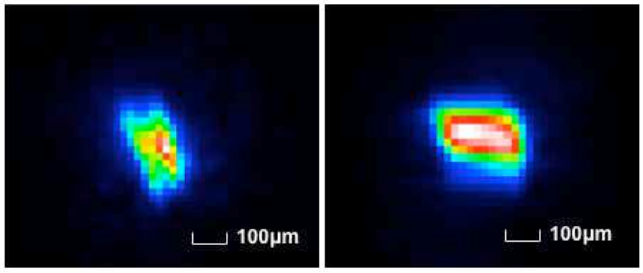

FIG. 3: XUV spots generated in Ar, with a slit aperture of 200 μm. (left) XUV spot of the 23$^{\rm rd}$ harmonic with OPG G400 grating, and size 140 μm x 220 μm.; (right) XUV spot of the 25$^{\rm th}$ harmonic with CG G1200 grating and size 220 μm x 120 μm. All spots have been acquired using a CCD camera (PIXIS-XO: 400B by Princeton Instruments, with resolution 20 μm).

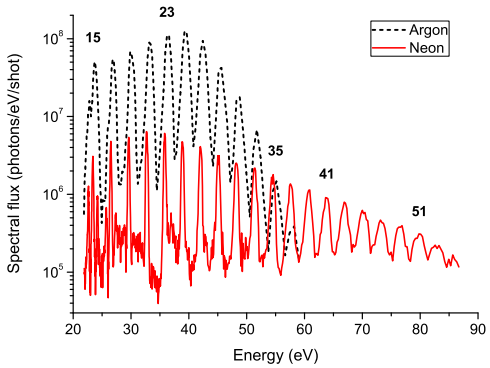

FIG. 4: Harmonic spectra generated in Ar and Ne using laser pulses with energy $\simeq$ 2 mJ, duration 40 $\pm$ 2fs (after transport to the generation chamber), wavelength = 805 nm and repetition rate = 5 kHz. Some of the harmonics have been labeled (see also Table II). The spectra have been acquired with a NIST-calibrated Al photodiode, placed at the exit of the monochromator. The monochromator slits aperture was set to 15 μm, in order to get a spectral resolution of about 0.05nm.

Two typical spectra, obtained using Ar and Ne for harmonic generation, are shown in Fig.4.

The use of Ar produced harmonics in the photon energy range 20-54 eV, with a peak of about $1 \cdot 10^8$ photons/pulse at about 40 eV (25$^{\rm th}$ harmonic). Using Ne, the plateau region moves towards higher energies, but with significantly reduced efficiency. In table 2 the generation efficiencies for the two gases at different harmonic orders are reported.

In the following two sections, we report the results of two pump-probe experiments carried out to characterize the source performance. The experiment described in Section III A aimed at measuring the duration of harmonic pulses transmitted by the monochromator. The experiment described in Section III B aimed at demonstrating the possibility of using CITIUS for studies of ultra-fast dynamics.

TABLE II: Generation efficiency after the monochromator with Ar and Ne. Selected harmonic orders are reported. In particular, the 35$^{\rm st}$ (54.25 eV) and 41$^{\rm st}$ (63.55 eV) harmonics generated with Ne, which correspond to the $M_{2,3}$ edges of Fe and Ni, respectively.

	15$^{\rm st}$ ph/pulse	23$^{\rm st}$ ph/pulse	35$^{\rm st}$ ph/pulse	41$^{\rm st}$ ph/pulse	51$^{\rm st}$ ph/pulse
Ar	$3.4 \cdot 10^7$	$1.1 \cdot 10^8$	$2.2 \cdot 10^6$	negligible	negligible
Ne	$7.1 \cdot 10^5$	$2.2 \cdot 10^6$	$1.5 \cdot 10^6$	$1.1 \cdot 10^6$	$5.6 \cdot 10^5$

A. Characterization of harmonic pulse duration

The pulse duration of HHG XUV pulses has been measured by means of an experiment based on LAPE (Laser Assisted Photoelectric Effect). This technique, described in detail in [20, 21], is based on the cross correlation of XUV and IR photons. In essence, the primary photoelectron spectrum resulting from XUV ionization of a target gas (Kr, in the case under scrutiny) is modified if the ionization takes place in the presence of a high-intensity laser pulse: the absorption and emission of laser photons gives rise to so-called sidebands in the photoelectron spectrum. The amplitude of the sidebands as a function of the delay between the XUV and IR pulses provides a cross-correlation signal from which one can extract the duration of XUV pulses.

The experiments were performed using the original hemispherical Scienta SES-200 electron spectrometer that was described in detail in [22]. The instrument consists of an accelerating-retarding multi-element electron lens and a hemispherical analyzer with 200 mm mean radius. It was installed at the CITIUS light source so that the electron lens collected electrons ejected in the dipole plane (i.e. perpendicular to the photon propagation vector) at an angle of 54.7 degrees from the horizontal direction. The choice of this angle guarantees electron intensities that are independent of the angular asymmetry parameter β, when horizontally linearly polarized radiation is used. Due to higher photon-flux transmission of the monochromator for vertically polarized HHG light, the reported measurement was carried out in this configuration. In this case, the β parameters of different transitions influence the observed relative intensities, but the effect can be expected to be of minor importance for the Kr $4p_{3/2}$ and $4p_{1/2}$ photoelectron lines. In any case, the polarization influence is irrelevant for the extraction of the photon temporal profile. In the chosen experimental configuration (i.e., pass energy of 50 eV), the resulting analyzer kinetic energy resolution was about 150 meV.

The choice of Kr for the LAPE experiment was mainly dictated by instrumental reasons. The 15th harmonic (23.22 eV) has sufficient energy to ionize the Kr 4p levels and is efficiently transmitted by all monochromator

gratings in the OPG configuration, with high-enough resolving power to fully resolve the $4p_{3/2}$ and $4p_{1/2}$ photoelectron lines. Additionally, the high photoionization cross section of Kr 4p electrons grants fast acquisition times. The laser pulse duration was carefully measured using a commercial autocorrelator and set at its minimum value, i.e., about 40 ± 2 fs after transport in the experimental chamber. The IR pulse was attenuated down to 80-100 mW in order to avoid saturation effects. Figure 5 shows a series of Kr 4p photo-electron spectra (horizontal axis), as a function of the delay between XUV and IR pulses (vertical axis). The relatively high flux produced by the source in this energy range allows to record each photo-electron spectrum in few minutes, while the measurements as a function of the delay lasted about one hour. The measurements have been performed using the G200 grating (see Table I). The two main photoelectron peaks, generated by the $4p_{3/2}$ and $4p_{1/2}$ states, have kinetic energies of 8.6 and 9.3 eV respectively. The presence of these peaks is due to a single-photon photoionization process and does not depend on the presence of the IR pulse. When the two pulses are temporally overlapped, two sidebands appear, corresponding to absorption and emission of one IR photon: these sidebands are at 7.8 and 10.8 eV for the $4p_{3/2}$ state, and at 7.1 and 10.1 eV for the $4p_{1/2}$ state. The intensity of each sideband as a function of the delay is the convolution of the XUV and IR pulses. The duration of the XUV pulse is obtained by deconvolving the IR signal from the Gaussian fit of the measured intensity. The black dots represent the temporal profile of the sideband at 10.8 eV; the solid line is a Gaussian fit.

The extracted pulse durations, the calculated energy resolution and the energy resolution corresponding to the Fourier limit of the 15$^{\text{th}}$ harmonic at the monochromator output are reported in Table III, for two gratings in OPG and one in CG. Since the beam divergence at H15 has been measured to be 1.3 mrad FWHM, it is possible to calculate the illuminated area on the grating and the respective expected pulse front-tilts. The obtained values for the OPG G200, OPG G400 gratings are, respectively, 18 and 36 fs, while for the CG G300 grating we found 125 fs. In the case of the OPG, the agreement between measurements and calculations is really good. In the case of CG, the measurements give an actual duration at the output that is longer than expected. This has been ascribed to a difference between the expected and the actual included angle of the CG stage. Anyway, the measurements confirm the capability of the monochromator to operate in two different regimes, either ultrafast response and low-energy resolution (i.e., OPG) or longer response and high-energy resolution (i.e., CG).

B. Ultrafast demagnetization of permalloy

In this section, we report the results of a pump-probe experiment demonstrating the possibility of using CITIUS to study the ultra-fast dynamics of selected chemical species, with a temporal resolution of few tens of femtoseconds.

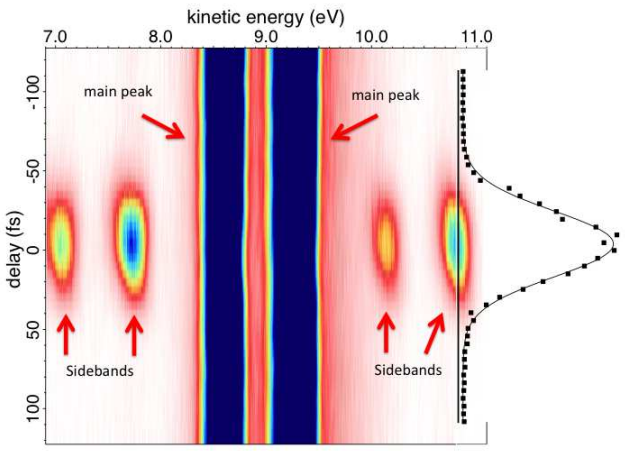

FIG. 5: Kr 4p photo-electron spectra obtained by overlapping the XUV (pump) and IR (probe) beams. In this case, the XUV beam (15th harmonic of the fundamental) was monochromatized by the G200 grating (OPG geometry, see Table 1). The black dots represent the integrated intensity of the sideband at 10.8 eV, as a function of the pump-probe delay; the solid line is a Gaussian fit. The pulse duration is obtained by deconvolving the contribution of the IR pulse from the measured profile.

TABLE III: Measured FWHM pulse duration, calculated spectral resolution (corresponding to a slit aperture of 100 μm) and energy resolution at the Fourier limit of the 15$^{\text{th}}$ harmonic (23.2 eV), transmitted by the monochromator in the OPG or CG stage.

Grating	Duration	Energy resolution	Fourier limit
OPG G200	23 ± 1.2 fs	0.5 eV	0.08 eV
OPG G400	35 ± 1.7 fs	0.25 eV	0.052 eV
OPG G600	35 ± 1.9 fs	0.16 eV	0.052 eV
CG G300	170 ± 10 fs	0.03 eV	0.01 eV

The spectral range covered by CITIUS includes the $M_{2,3}$ thresholds of transition metals (54.25 eV, i.e., the 35$^{\text{th}}$ harmonic of the fundamental, see Table II), making CITIUS an appealing source for the study of magnetic materials. As a proof-of-principle application, we measured the demagnetization of a 100 mm thick permalloy film ($Fe_{20}Ni_{80}$), using X-ray resonant magnetic scattering [23, 24] in pump-probe configuration.

The experiment was performed using the IRMA reflectometer [25]. The instrument permits to precisely adjust the angles between the sample surface and the incoming/reflected XUV beam. Three photodiodes and one channel electron multiplier are mounted on the detector arm. By means of a horseshoe electromagnet, it is possible to apply a variable magnetic field up to ±1500 Oe,

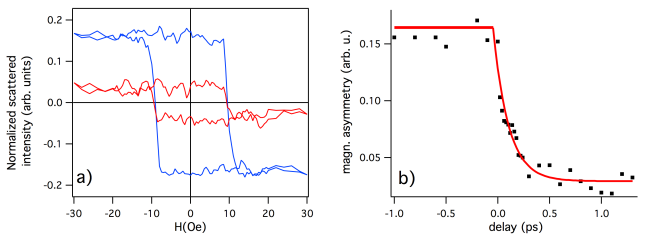

FIG. 6: a) Hysteresis loops measured at the 35$^{\text{th}}$ harmonic of the fundamental ($M_{2,3}$ thresholds of transition metals) for HHG pulse arriving 1 ps before (blue line) and 1 ps after (red line) the IR pump pulse. b) Pump-probe delay dependency of the magnetic asymmetry ratio at saturation (dots) and exponential decay fit. The magnetization quenching is about 80 % after 0.5 ps and the characteristic decay time is 0.21 ± 0.02 ps.

parallel to the sample surface. The scattering experiment was conducted in a transverse MOKE-like configuration [26]. In this configuration, using p-polarized XUV light, one is sensitive to the magnetization component perpendicular to the scattering plane. Moreover, choosing the incoming/scattering angle close to the Brewster condition (about 45 deg at 54 eV), the magnetization contrast is maximized with respect to the (strongly suppressed) non-magnetic scattered background, thus improving the signal-to-noise ratio of the measurement.
We have measured the magnetic hysteresis loop at the Fe $M_{2,3}$ edge, as a function of the delay between the transmitted IR beam (pump) and the XUV pulse (probe). Figure 6a shows the hysteresis loop when the XUV pulse arrives on the sample 1 ps before (blue curve) and 1 ps after (red curve) the IR pulse. Each hysteresis loop was recorded in few minutes. The plots are normalized to the average scattered intensity. The magnetic asymmetry ratio is defined as $(I_+ - I_-)/(I_+ + I_-)$, where I_+ and I_- denote the intensities of the reflected light as the externally applied magnetic field is reversed in direction. In Fig.6b, the asymmetry ratio at saturation is plotted as a function of the pump-probe delay. Data show the ultrafast demagnetization of the Fe atoms of the sample. Almost 80 % of the magnetization is dissipated 0.5 ps after the sample has been illuminated with the IR pulse. The data have been fitted with an exponential decay curve, indicating a characteristic demagnetization time of 0.21 ± 0.02 ps. Despite the modest scientific interest of this particular sample, which has been already investigated in detail by other groups [3, 27], these results demonstrate that our apparatus is capable of measuring the ultrafast magnetization dynamics of selected chemical species, with a resolution of few tens of femtoseconds.

IV. CONCLUSIONS AND FUTURE DEVELOPMENTS

We have presented the characteristics of CITIUS, a new IR-XUV, femtosecond, Italo-Slovenian light source, based on laser-induced high-harmonic generation in gas. As a next step, we will carry out the commissioning of the experimental equipment for time resolved photoemission investigations. The apparatus consists of two vacuum chambers equipped with two different electron spectrometers: an Angle-Resolved Time of Flight (VG-Scienta ARToF 10k) for pump-probe experiments and an hemispherical spectrometer (VG-Scienta R3000), which will be used in combination with a monochromatized twin anode X-ray source for conventional X-ray photoemission spectroscopy measurements. A preparation chamber, equipped with evaporators and standard sample preparation tools, such as sample heating, ion sputtering and LEED, will connect the two chambers. The sample will be hosted on a cryo-manipulator (able to reach a temperature below 10 K), operated with liquid helium, with five degrees of freedom.
Starting from 2014, the source will be open to external users, interested in developing time-resolved applications in different domains of both fundamental and applied science. Envisaged experiments will be in particular related to photophysics and photochemistry, including materials science, catalysis, magnetism and biochemistry. Part of the activity will be carried out in close connection with that developed at the Low-Density Matter beamline of the FERMI free-electron laser.

V. ACKNOWLEDGEMENTS

The CITIUS project is funded by the program for cross-border cooperation between Italy and Slovenia 2007-2013. C. Grazioli gratefully acknowledges financial support through the TALENTS Programme (7th Framework Programme, Specific Programme: PEOPLE - Marie Curie Actions - COFUND). We aknowledge the Department of Physics and Astronomy of Uppsala University for providing the Scienta SES-200 spectrometer, in the framework of the collaboration with CNR-IOM (TASC laboratory, Gas Phase beamline, Trieste). We also thank Carla Puglia and Monica de Simone for technical assistance in setting up the photoemission experimental set-up, and Sandra Gardonio for valuable suggestions about the source desing. G.D.N. is particularly thankful to Gvido Bratina for technical and moral support during the preparation and implementation of the project CITIUS.

[1] T. Pfeifer, C. Spielmann and G. Gerber, *Rep. Prog. Phys.* **69**, 604 (2006).
[2] Zewail, *J. Phys. Chem. A* **104**, 5660 (2000).
[3] La-O-Vorakiat et al., *Phys. Rev. Lett.* **103**, 257402

(2009).
[4] N. L. Wagner et al., *P. Natl. Acad. Sci. USA* **103**, 13279 (2006).
[5] P. B. Corkum, *Phys. Rev. Lett.* **71**, 143903 (1993).
[6] Z.H. Chang et al., *Phys. Rev. Lett.* **79**, 2967 (1997).
[7] C. Spielmann et al., *Science* **278**, 661 (1997).
[8] E. Seres et al., *Phys. Rev. Lett.* **92**, 163002 (2004).
[9] http://www.ita-slo.eu.
[10] B.Frietsch et al., *Rev. Sci. Instrum.* **84**, 075106 (2013).
[11] L. Dakovski et al., *Rev. Sci. Instrum.* **81**, 073108 (2010).
[12] S. Mathias et al., *Rev. Sci. Instrum.* **78**, 083105 (2007).
[13] L. Nugent-Glandorf et al., *Rev. Sci. Instrum.* **78**, 1875 (2002).
[14] http://www.elettra.trieste.it/it/lightsources/fermi/fermi-beamlines/ldm/ldmhome-page.html.
[15] L. Poletto et al., *Rev. Sci. Inst.* **80**, 123109 (2009).
[16] F. Frassetto et al., *Opt. Express* **19**, 19169 (2011).
[17] H. Igarashi et al., *Opt. Express* **20**, 3725 (2012).
[18] L. Poletto and F. Frassetto, *Appl. Opt.* **49**, 5465 (2010).
[19] L. Poletto and F. Frassetto, *Applied Sciences* **3**, 1 (2013).
[20] T. E. Glover et al., *Phys. Rev. Lett.* **76**, 2468 (1996).
[21] E. S. Toma et al., *Phys. Rev. A* **62**, 061801 (2000).
[22] N. Mårtensson et al., *J. Electron Spectrosc. Relat. Phenom.* **70**, 117 (1994).
[23] D. Gibbs et al., *Phys. Rev. Lett.* **61**, 1241 (1998).
[24] J. P. Hannon et al., *Phys. Rev. Lett.* **61**, 1245 (1998).
[25] M. Sacchi et al., *Rev. Sci. Instrum.* **74**, 2791 (2003).
[26] P. N. Argyres, *Phys. Rev.* **97**, 334 (1955).
[27] E. Beaurepaire et al., *Phys. Rev. Lett.* **76**, 4250 (1996).